

Fullerene-like models for microporous carbon: a review

Article

Accepted Version

Harris, P. (2013) Fullerene-like models for microporous carbon: a review. *Journal of Materials Science*, 48 (2). pp. 565-577. ISSN 1573-4803 doi: <https://doi.org/10.1007/s10853-012-6788-1> Available at <https://centaur.reading.ac.uk/28956/>

It is advisable to refer to the publisher's version if you intend to cite from the work. See [Guidance on citing](#).

To link to this article DOI: <http://dx.doi.org/10.1007/s10853-012-6788-1>

Publisher: Springer

Publisher statement: The original publication is available at www.springerlink.com

All outputs in CentAUR are protected by Intellectual Property Rights law, including copyright law. Copyright and IPR is retained by the creators or other copyright holders. Terms and conditions for use of this material are defined in the [End User Agreement](#).

www.reading.ac.uk/centaur

CentAUR

Central Archive at the University of Reading

Reading's research outputs online

Fullerene-like models for microporous carbon: A review

Peter J.F. Harris*

Centre for Advanced Microscopy, J.J. Thomson Physical Laboratory, University
of Reading, Whiteknights, Reading RG6 6AF, UK.

*Corresponding author. Tel/Fax: +44 118 378 6118.

E-mail address: p.j.f.harris@reading.ac.uk

Abstract

Microporous carbons are important in a wide variety of applications, ranging from pollution control to supercapacitors, yet their structure at the molecular level is poorly understood. Over the years, many structural models have been put forward, but none have been entirely satisfactory in explaining the properties of the carbons. The discovery of fullerenes and fullerene-related structures such as carbon nanotubes gave us a new perspective on the structure of solid carbon, and in 1997 it was suggested that microporous carbon may have a structure related to that of the fullerenes. Recently, evidence in support of such a structure has been obtained using aberration-corrected transmission electron microscopy, electron energy loss spectroscopy and other techniques. This article describes the development of ideas about the structure of microporous carbon, and reviews the experimental evidence for a fullerene-related structure. Theoretical models of the structural evolution of microporous carbon are summarised, and the use of fullerene-like models to predict the adsorptive properties of microporous carbons are reviewed.

Keywords: Microporous carbon, fullerenes, transmission electron microscopy, adsorption

Contents

1.	Introduction.....	3
2.	Graphitizing and non-graphitizing carbons	5
3.	Structure of non-graphitizing carbon: early work	6
4.	Structure of non-graphitizing carbon: fullerene-related models	9
5.	Experimental evidence for fullerene-related structure of non-graphitizing carbon	12
6.	Modelling the structural evolution of microporous carbon	14
7.	Modelling adsorption using fullerene-like models for microporous carbon	16
8.	Discussion	19
	Acknowledgements	22
	References.....	22

1. Introduction

The adsorptive properties of charcoal have been known for thousands of years. Egyptian papyri from 1500BC record the application of charcoal to adsorb odorous vapours from putrefying wounds, while Hindu documents from 450 BC refer to the use of sand and charcoal filters for the purification of drinking water [1]. In the 18th century, charcoal began to be used industrially for the decolourization of sugar syrups, while in the First World War the deployment of poisonous gases created an urgent need for adsorbent carbons suitable for use in respirators. Today, activated microporous carbon is used on an enormous scale for the purification of air and water [2,3]. It is still used widely in respirators, as well as in air-conditioning systems and in

1 the clean-up of waste gases from industry. In the liquid-phase, its largest
2 single application is the removal of organic contaminants from drinking water.
3
4 Many water companies in Europe and the USA now filter all domestic supplies
5 through granular activated carbon filters, and household water filters
6
7 containing activated carbon are also in widespread use. Other applications
8
9 include decontamination of groundwaters and control of automobile
10
11 emissions. Microporous carbon is also an important support material in
12
13 heterogeneous catalysis, and is used in lithium ion batteries and
14
15 supercapacitors. As a result of its commercial importance, charcoal has been
16
17 the subject of a huge amount of research in both industrial and academic
18
19 laboratories. Despite this, many important questions remain, not least about
20
21 its detailed atomic structure.
22
23
24
25
26
27
28
29
30

31 The primary aim of this article is to discuss the idea, first put forward by the
32 present author and S.C. Tsang in 1997 [4,5], that charcoal, or char, has a
33
34 structure related to that of the fullerenes. In order to put this in context, a brief
35
36 outline of earlier work in the field is included. The article begins with a brief
37
38 description of the characteristics of graphitizing and non-graphitizing carbons,
39
40 and highlights the work of Rosalind Franklin in establishing the distinction
41
42 between these two forms of carbon. Some of the structural models which
43
44 have been put forward for non-graphitizing carbons are then discussed,
45
46 beginning with Franklin's original models, which were based on cross-linked
47
48 graphitic domains. Subsequent workers suggested that sp^3 -bonded carbon
49
50 atoms might be present in the cross-links, while later workers interpreted
51
52 transmission electron microscopy (TEM) images of microporous carbon in
53
54
55
56
57
58
59
60
61
62
63
64
65

terms of a ribbon-like structure. The studies which led to the proposal of the fullerene-related model are then outlined, and experimental support for this structure is discussed. The strongest experimental support comes from studies carried out in the past four years using aberration-corrected TEM and electron energy loss spectroscopy (EELS). Both techniques provide evidence for the presence of pentagonal carbon rings in microporous carbon.

In the subsequent section, some attempts to model the structural evolution of microporous carbon are reviewed. It is notable that in each case these modelling exercises lead to structures which contain non-hexagonal rings. Finally, the use of fullerene-like models of microporous carbons to predict their adsorptive properties is summarised.

2. Graphitizing and non-graphitizing carbons

In the early part of the 20th century it was established that carbons formed by the pyrolysis of organic materials fall into two distinct classes, cokes and chars. The two types of carbon have quite different physical properties. Cokes are relatively dense and soft whereas chars are hard, low density materials. Although cokes may be porous, this porosity is on a relatively large scale. Chars, on the other hand, have a high degree of microporosity, although some of this porosity is usually inaccessible to gases. The internal surface area can be enhanced by activation, i.e. mild oxidation with a gas such as carbon dioxide, steam or air. In this way surface areas of the order of $2000 \text{ m}^2 \text{ g}^{-1}$ can be achieved. There is another key distinction between cokes and chars: the former can be converted into graphite by high temperature annealing while the

latter cannot. It is not entirely clear when this was first demonstrated, but it was certainly known in the 1940s. In a major review article published in 1948 [6], Paul Emmett describes work carried out by H.F. Johnston and G.L. Clark, who showed that “charcoals sinter and turn into graphite much less readily than does petroleum coke”. Unfortunately this work only seems to have been published in US government reports. The first detailed study of this topic to appear in the open literature is Rosalind Franklin’s classic 1951 paper [7]. Franklin prepared carbons from a wide range of organic materials, including sugar, polyvinylidene chloride (PVDC), polyvinyl chloride (PVC) and pitch. She then used X-ray diffraction to investigate the effect of heat treatment, up to a temperature of 3000 °C, on the structure of these carbons. She found that some of the carbons, including those prepared from PVC and pitch could be graphitized by heat treatments above about 2200 °C, while others, such as those prepared from sugar and PVDC, could not be transformed into crystalline graphite, even at 3000 °C. Instead, they formed a porous, isotropic material which only contained tiny domains of graphite-like structure. Franklin coined the terms “graphitizing” and “non-graphitizing” to describe these two classes of carbon.

3. Structure of non-graphitizing carbon: early work

In his 1948 review Paul Emmett stated that “There are very few things about which we can be sure as regards the structure of charcoal.” However, he goes on to express the view that “The X-ray results taken as a whole constitute strong evidence that much of the carbon in charcoal is arranged in platelets”. Emmett’s idea seems to be that char consists of tiny flakes of graphene

1 approximately aligned with each other, giving a structure in which the pores
2 have a slit-like shape. This picture of porosity in carbon as a system of
3 interconnecting slits has proved extremely tenacious. In fact, it is still used in
4 theoretical studies of adsorption and permeability of carbons [e.g. 8,9].
5
6 However, there is little experimental evidence that the pores in non-
7
8 graphitizing carbon are generally slit-like in shape. Franklin's 1951 X-ray
9
10 diffraction study demonstrated rather the opposite, as can be seen from Fig.
11
12 1, which shows her models for non-graphitizing and graphitizing carbons. In
13
14 these models, the basic units are small graphitic crystallites containing a few
15
16 layer planes, which are joined together by cross-links. For the non-graphitizing
17
18 carbon (Fig. 1(a)), the structural units are oriented randomly, so that the
19
20 structure is isotropic, while in the graphitizing carbon (Fig. 1(b)) the units are
21
22 approximately parallel to each other. It is clear that the structure in Fig. 1(b) is
23
24 more amenable to transformation into graphite.
25
26
27
28
29
30
31
32
33
34
35

36 Franklin's ideas on graphitizing and non-graphitizing carbons are probably
37
38 broadly correct, but they are in some regards incomplete. For example, the
39
40 nature of the cross-links between the graphitic fragments is not specified, so the
41
42 reasons for the sharply differing properties of graphitizing and non-graphitizing
43
44 carbons is not explained. Some authors have suggested that the "cross-links"
45
46 envisaged by Franklin might in fact be sp^3 -bonded atoms [e.g. 10]. The
47
48 presence of diamond-like domains would be consistent with the hardness of
49
50 non-graphitizing carbons, and might also explain their extreme resistance to
51
52 graphitization. A problem with these models is that sp^3 carbon is unstable at
53
54 high temperatures: diamond is converted to graphite at 1700°C. Therefore, the
55
56
57
58
59
60
61
62
63
64
65

1 presence of sp^3 atoms in a carbon is unlikely to explain the resistance of the
2 carbon to graphitization at high temperatures, although the presence of small
3 amounts of sp^3 carbons cannot be ruled out. It should also be noted that
4 diffraction studies of non-graphitizing carbons have found no evidence for the
5 presence of sp^3 -bonded atoms [11].
6
7
8
9
10

11
12
13
14 Transmission electron microscopy began to play a major role in the structural
15 study of carbon in the 1970s, when improvements in lens design meant that
16 the interlayer (0.34 nm) graphitic spacing could be readily resolved [12]. In
17 1975, Ban, Crawford and Marsh described a lattice-resolution TEM study of
18 non-graphitizing carbons derived from polyvinylidene chloride [13]. The
19 structures of the carbons following heat treatments at temperatures in the range
20 530 °C - 2700 °C was investigated. Images of these carbons apparently showed
21 the presence of curved graphite sheets, typically two or three layer planes thick,
22 enclosing voids. These images led Ban *et al.* to suggest that heat treated non-
23 graphitizing carbons have a ribbon-like structure. A rather similar model for the
24 structure of glassy carbon had been proposed by Jenkins and Kawamura in
25 1971 [14]. However, models of this kind have serious weaknesses. Such models
26 consist of curved and twisted graphene sheets enclosing irregularly-shaped
27 pores. However, graphene sheets are known to be highly flexible, and would
28 therefore be expected to become ever more closely folded together at high
29 temperatures, in order to reduce surface energy. Indeed, tightly folded graphene
30 sheets are quite frequently seen in carbons which have been exposed to
31 extreme conditions. Thus, structures like the ones envisaged by Jenkins, Ban
32 and their colleagues would be unlikely to be stable at very high temperatures. It
33
34
35
36
37
38
39
40
41
42
43
44
45
46
47
48
49
50
51
52
53
54
55
56
57
58
59
60
61
62
63
64
65

has also been pointed out by Oberlin [15] that the ribbon-like models are based on a questionable interpretation of the electron micrographs. In most micrographs of graphitized carbons, only the {002} fringes are resolved, and these are only visible when they are approximately parallel to the electron beam. Therefore, such images tend to have a ribbon-like appearance. However, since only a part of the structure is being imaged, this appearance can be misleading, and the true three-dimensional structure may be more cage-like than ribbon-like.

4. Structure of non-graphitizing carbon: fullerene-related models

The discovery of the fullerenes [16 - 18] and subsequently of related structures such as carbon nanotubes [19,20] and nanohorns [21,22], has given us a new paradigm for solid carbon structures. We now know that carbons containing pentagonal rings, as well as other non-six-membered rings, among the hexagonal sp^2 carbon network, can be highly stable. This new perspective prompted a number of groups to take a fresh look at well-known forms of carbon, to see whether any evidence could be found for the presence of fullerene-like structures.

The first studies to consider the idea that non-graphitizing, microporous carbon might have a structure related to that of the fullerenes were published in 1997 [4,5]. A series of subsequent papers developed the idea further [23 - 26]. In the original studies, some non-graphitizing carbons were examined using transmission electron microscopy before and after heat treatments at very high temperatures (up to 2600 °C). For comparison, graphitizing carbons treated in a similar way were also examined. Typical TEM micrographs of non-graphitizing

1 and graphitizing carbons prepared at 1000 °C are shown in Fig. 2. The insets
2 show diffraction patterns recorded from areas approximately 0.25 μm in
3 diameter. The image of the non-graphitizing carbon shows the structure to be
4 disordered and isotropic, consisting of tightly curled single carbon layers, with no
5 obvious graphitization. The diffraction pattern shows symmetrical rings,
6 confirming the isotropic structure. The appearance of graphitizing carbon, on the
7 other hand, approximates much more closely to that of graphite. In this case the
8 structure contains small, approximately flat carbon layers, packed tightly
9 together with a high degree of alignment. The fragments can be considered as
10 rather imperfect graphene sheets. The diffraction pattern for the graphitizing
11 carbon consists of arcs rather than symmetrical rings, confirming that the layers
12 are preferentially aligned along a particular direction. The bright, narrow arcs in
13 this pattern correspond to the interlayer {002} spacings, while the other
14 reflections appear as broader, less intense arcs.

35
36 Micrographs showing the effect of high temperature heat treatments on the
37 structure of non-graphitizing and graphitizing carbons are shown in Fig. 3 (note
38 that the magnification here is much lower than for Fig. 2). In the case of the non-
39 graphitizing carbon, heating at 2300 °C in an inert atmosphere produces the
40 disordered, porous material shown in Fig. 3 (a). This structure is made up of
41 curved and faceted graphitic layer planes, typically 1 - 2 nm thick and 5 – 15 nm
42 in length, enclosing randomly-shaped pores. A few somewhat larger graphite
43 crystallites are present, but there is no macroscopic graphitization. In contrast,
44 heat treatment of the anthracene-derived carbon produces large crystals of
45 highly ordered graphite, as shown in Fig. 3 (b).

1
2 More detailed analysis of the heat-treated non-graphitizing carbons showed that
3
4 they often contained closed nanoparticles; examples can be seen in Fig. 4. The
5
6 particles were usually faceted, and often hexagonal or pentagonal in shape.
7
8 Sometimes, faceted layer planes enclosed two or more of the nanoparticles, as
9
10 shown in Fig. 4 (b). Here, the arrows indicate two saddle-points, which are
11
12 indicative of heptagonal rings, as pointed out by Iijima and colleagues [27]. The
13
14 closed nature of the nanoparticles, their hexagonal or pentagonal shapes, and
15
16 other features such as the saddle-points strongly suggest that the particles have
17
18 fullerene-like structures. Indeed, in many cases the particles resemble those
19
20 produced by arc-evaporation in a fullerene generator although in the latter case
21
22 the particles usually contain many more layers.
23
24
25
26
27
28
29
30

31 The observation of fullerene-related nanoparticles in the heat treated carbons
32
33 suggested that the original, freshly-prepared carbons may also have had
34
35 fullerene-related structures. This prompted the present author and colleagues to
36
37 propose a model for the structure of non-graphitizing carbons which consists of
38
39 discrete fragments of curved carbon sheets, in which pentagons and heptagons
40
41 are dispersed randomly throughout networks of hexagons, as shown in Fig. 5. It
42
43 should be noted that this representation of the structure is intended as an
44
45 illustration, rather than a full, three-dimensional model. In subsequent work,
46
47 discussed in section 7, three-dimensional structures have been created from the
48
49 curved fragments, and have been used to model adsorption.
50
51
52
53
54
55
56
57
58
59
60
61
62
63
64
65

5. Experimental evidence for fullerene-related structure of non-graphitizing carbon

The micrographs shown in Figs. 2, 3 and 4 were recorded using conventional transmission electron microscopy. The resolution achievable with such microscopes is typically around 0.18 nm. In the past 10 years or so, a new generation of TEMs has become available with resolutions of 0.05 nm or better. This has been achieved through the use of aberration-correctors, which compensate for the inherent defects of electron lenses [28]. These microscopes are capable of resolving carbon atoms in graphene, where the atomic spacing is 0.142 nm [29, 30]. In 2008, Suenaga, Liu and the present author applied this technique for the first time to a microporous carbon [31]. The carbon studied was a commercial activated carbon, Norit GSX. Imaging was carried out in an aberration-corrected TEM operated at 120kV, with a point resolution of better than 0.14 nm. Obtaining atomic resolution images of the fresh carbon proved to be extremely challenging, and the images which were recorded were difficult to interpret. A typical example is shown in Fig. 6. At the edge of this fragment the individual rings of carbon atoms are resolved: the bright spots represent the centres of the rings. In some cases, pentagonal arrangements of spots can be discerned: an example is arrowed. However, the images of the fresh carbon were not of sufficient quality to provide definite proof of the presence of pentagons.

Much better quality images could be obtained from carbon samples which had been heated at high temperature, in order to increase the crystallinity. An image from a carbon sample which had been heated in Ar to 2000 °C is shown

1 in Fig. 7 (a). Here there is clear evidence for the presence of five-membered
2 rings. The area enlarged in Fig. 7 (b) shows an arrangement of 5 bright spots
3 surrounding a central spot. A good match was obtained with the simulated
4 image in Fig. 7 (c), which was obtained from the structure in Fig. 7 (d) using a
5 standard multi-slice procedure. Here, the pentagon is oriented approximately
6 parallel to the plane of the image. A second area which contains a pentagonal
7 structure is shown in Fig. 7 (e). In this case the central pentagonal ring is not
8 visible, apparently because the ring is tilted away from the plane of the image.
9 Support for this comes from the reasonable match which can be seen
10 between the image and the simulated image in Fig. 7 (f), obtained from the
11 structure in Fig. 7 (g). Images of this kind provide convincing evidence for the
12 presence of pentagonal carbon rings in the heat-treated carbon.
13
14
15
16
17
18
19
20
21
22
23
24
25
26
27
28
29
30

31 In addition to high resolution imaging, TEM can also probe the structure of
32 material through the use of electron energy loss spectroscopy (EELS). In 2011,
33 Zhang *et al.* used EELS to investigate the structure of a non-graphitizing
34 carbon derived from phenolic resin [32]. In this study a detailed analysis was
35 carried out of the carbon K-edge spectrum. When the C=C π^* , C—C σ^* and
36 C=C σ^* components were removed from the spectrum, a residual feature was
37 found between 286 and 288 eV. A similar feature is observed in spectra
38 recorded from crystalline C₆₀ [33] and could therefore be interpreted as
39 evidence for five-membered rings. As Zhang *et al.* point out, further theoretical
40 modelling would be valuable in confirming this interpretation.
41
42
43
44
45
46
47
48
49
50
51
52
53
54
55
56
57
58
59
60
61
62
63
64
65

Evidence for fullerene-like structures in microporous carbons has also been found using Raman spectroscopy. Burian, Dore and colleagues have used this method to analyse carbons prepared from sucrose, heat treated at temperatures from 1000 °C - 2300 °C [34, 35]. The Raman spectra showed clear evidence for the presence of fullerene- and nanotube-like elements in the carbons.

X-ray and neutron diffraction studies have generally been less useful than microscopy and spectroscopy in establishing whether microporous carbons have a fullerene-related structure, since the interpretation of diffraction data from these highly disordered materials is not straightforward. Burian, Dore and their co-workers have published a number of studies in this area [e.g. 36, 37] and have found that the results are consistent with the presence of non-six membered rings, but other interpretations may also be possible.

6. Modelling the structural evolution of microporous carbon

The formation mechanism of microporous carbon is not well understood at the atomic level. A number of groups have attempted to model the process, and in several cases these modelling exercises have produced structures which contain fullerene-like elements. One of the first such exercises was reported by Acharya *et al.* in 1999 [38]. In this work the carbon was assumed to be derived from polyfurfuryl alcohol. The starting point for the simulation was a series of all-hexagon fragments, terminated with hydrogens, as shown in Fig. 8 (a), while Figs. 8 (b) – (d) illustrate the evolution of the structure as the H/C ratio is reduced (i.e. the temperature is increased). During this evolution,

1 pentagons and heptagons form as well as hexagons, resulting in the formation
2 of curved fragments.
3
4
5
6

7 In a later study, Kumar *et al.* used Monte Carlo (MC) simulations to model the
8 evolution of a polymer structure into microporous carbon [39]. Again
9 polyfurfuryl alcohol was chosen as the precursor, and in this case the starting
10 structure was the polymer itself rather than hexagonal fragments of carbon.
11 Simulations were carried out with a number of different polymer starting
12 structures and different pre-defined densities. In each case the final carbon
13 was made up of a hexagonal network with 10-15 % non-hexagonal rings
14 (pentagons and heptagons). The properties of the simulated carbons
15 appeared to be generally consistent with experimental results.
16
17
18
19
20
21
22
23
24
25
26
27
28
29
30

31 A different approach to modelling the evolution of microporous carbon was
32 used by Shi [40]. Here, the initial system consisted of carbon gas atoms at
33 very high temperature. This choice of initial condition was intended to
34 represent the high temperature state in a pyrolysis process after the polymer
35 chains break down and most other elements have evaporated. The
36 temperature was then decreased so that the atoms “condensed” to form a
37 porous structure composed of curved and defected graphene sheets, in which
38 the curvature was induced by non-hexagonal rings.
39
40
41
42
43
44
45
46
47
48
49
50
51
52

53 In 2009, Powles, Marks and Lau described a comprehensive molecular-
54 dynamics study of the self-assembly of carbon nanostructures [41]. The
55 precursor for these simulations was highly disordered amorphous carbon, which
56
57
58
59
60
61
62
63
64
65

1 was generated by rapid quenching of an equilibrated liquid sample. It was found
2 that, under certain conditions, annealing the amorphous carbon at high
3
4 temperature could lead to the highly curved sp^2 sheet structure shown in Fig. 9.
5
6 The resemblance between this and the structure shown in Fig. 5 is very
7
8 striking.
9
10

11 12 13 14 **7. Modelling adsorption using fullerene-like models for microporous** 15 16 17 **carbon**

18
19 To date, there have been relatively few attempts to use fullerene-like models
20
21 to predict the adsorptive and other properties of microporous carbons. By far
22
23 the most ambitious programme of work in this area has been carried out by
24
25 Terzyk, Gauden and colleagues, whose results have been published in a
26
27 series of papers beginning in 2007 [42 - 49]. In the first of these [42], 36
28
29 different carbon structures with increasing microporosity, labelled S0 - S35,
30
31 were generated. The initial microporous structure, named S0, is shown in Fig.
32
33 10 (top left). Fragments were then progressively added to create the 36
34
35 structures labelled S0 - S35. Pore size distribution (PSD) curves for the
36
37 structures were calculated using the method of Bhattacharya and Gubbins
38
39 (BG) [50]. This involves determining the statistical distribution of the radii of
40
41 the largest sphere that can be fitted inside a pore at a given point. A selection
42
43 of the PSD curves determined in this way is shown in Fig. 11. It can be seen
44
45 that the most “crowded” structure, S35, has a much narrower range of pore
46
47 sizes than the initial S0 structure. Argon adsorption isotherms were simulated
48
49 for these structures using the parallel tempering Monte Carlo simulation
50
51 method developed by Yan and de Pablo [51]. Some of these isotherms are
52
53
54
55
56
57
58
59
60
61
62
63
64
65

1 shown in Fig. 12. These show that the gradual crowding of the S0 structure
2 (leading finally to S35) leads to a decrease in the maximum number of
3 adsorbed molecules. On the other hand, the S0 structure exhibits less
4 adsorption at low pressures than the more crowded ones because the
5 average micropore diameter is larger. Also notable is the increasing
6
7 “sharpness” of the inflection point in the isotherms, a feature which is often
8 reported for experimental systems (e.g. [52]). The simulated isotherms were
9 then used to determine PSD curves, using a range of widely used methods,
10 with the aim of checking the validity of these methods. Good agreement was
11 found between the PSDs determined from the isotherms and the PSDs from
12 the BG method. This confirms the validity of various methods for calculating
13 PSD curves from adsorption data. It would also seem to confirm the validity of
14 the fullerene-related model for microporous carbon.
15
16

17 In the next paper of this series [43], Terzyk *et al.* began with 3 structures
18 constructed from fullerene-like fragments, as shown in Fig. 13. The densities
19 of these structures were calculated, and values in the range 2.18 - 2.24 g cm⁻³
20 were found, consistent with typical densities of non-graphitizing carbons.
21 Once again, pore size distributions for the structures were determined using
22 the BG method. As in the previous paper, the simulated isotherms were used
23 to determine PSD curves, using a range of widely used methods. Good
24 agreement was found between the PSDs determined from the simulated
25 adsorption data and the original PSDs from the BG method. This is illustrated
26 in Fig. 14, where the PSD curve determined from the Bhattacharya-Gubbins
27 method is compared with results from the Horvath–Kawazoe method [53].
28
29
30
31
32
33
34
35
36
37
38
39
40
41
42
43
44
45
46
47
48
49
50
51
52
53
54
55
56
57
58
59
60
61
62
63
64
65

1
2 In a further paper [44], the adsorption of Ne, Ar, Kr, Xe, CCl₄ and C₆H₆ on the
3
4 S0 and S35 carbons was modelled. The simulated data were compared with
5
6 the predictions of the Dubinin–Radushkevich [54] and Dubinin–Astakhov [55]
7
8 adsorption isotherm equations, and a good fit was found for the S35 carbon.
9
10 For the S0 carbon the Dubinin–Izotova (DI) equation [56] gave a better fit
11
12 because the micropores in this model have a wide distribution of diameters.
13
14 The simulated isotherms exhibited a number of features similar to those seen
15
16 in experimental results. For example the isotherms for CCl₄ and C₆H₆ were
17
18 temperature invariant, as observed experimentally. It was also noted that the
19
20 isotherms obeyed Gurvich’s rule, which states that the larger the molecular
21
22 collision diameter the smaller the access to micropores, as well as other
23
24 empirical and fundamental correlations developed for adsorption on
25
26 microporous carbons.
27
28
29
30
31
32
33
34
35

36 The effect of oxidising the carbon surface on porosity was analysed in a paper
37
38 published in 2009 [45]. A “virtual oxidation” procedure was employed, in which
39
40 surface carbonyls were attached to carbon atoms located on the edges of the
41
42 fragments. It was assumed that the structure of the carbon skeleton remained
43
44 unchanged. Pore size distributions, determined using the BG method were
45
46 found not to be greatly affected by oxidation. Simulated isotherms for Ar, N₂
47
48 and CO₂ were calculated using the GCMC method. For Ar, the effect of
49
50 oxidation on the isotherm was relatively small. However, for N₂ and CO₂ there
51
52 were significant changes in the isotherms, due to electrostatic interactions
53
54 between N₂ and CO₂ and the surface carbonyl groups. As a consequence of
55
56
57
58
59
60
61
62
63
64
65

1 this, pore size distributions calculated from the simulated isotherms for N₂ and
2 CO₂ differed markedly from those originally determined from the BG method.
3
4 An important conclusion from this is that experimental PSDs determined using
5 CO₂ (or using N₂ if there is a large oxygen content) may be unreliable. A
6
7 further study looked at the influence of carbon surface oxygen groups on
8
9 Dubinin-Astakhov equation parameters calculated from CO₂ isotherms [46]. It
10
11 was concluded that porosity parameters calculated by fitting the DA model to
12
13 experimental CO₂ adsorption data may be questionable.
14
15
16
17
18
19
20
21

22 Terzyk and colleagues have published a number of other studies in which
23
24 fullerene-like models have been used to predict the properties of microporous
25
26 carbons [47 - 49], but the results summarised above are sufficient to
27
28 demonstrate the utility of such models.
29
30
31
32
33
34
35

36 **8. Discussion**

37 The structure of microporous carbon has been a subject of uncertainty for
38
39 decades, and a wide range of different structural models have been proposed.
40
41 The idea discussed in this review, that microporous carbon has a structure
42
43 related to that of the fullerenes, is by no means universally accepted, and will
44
45 remain controversial until unequivocal experimental evidence is obtained. The
46
47 best hope of achieving such proof probably lies with aberration-corrected
48
49 transmission electron microscopy. As discussed in Section 5, the advent of this
50
51 new form of TEM has meant that directly imaging the ring structure of graphitic
52
53 carbons is now a practical possibility. Initial studies using this technique [31]
54
55
56
57
58
59
60
61
62
63
64
65

1 have produced convincing evidence for pentagonal rings in carbon heated to
2 2000 °C, but further work is needed to achieve clear images of pentagons in
3
4 “fresh” carbon. This is clearly a considerable experimental challenge, but not
5
6 beyond the capabilities of current microscopes.
7
8
9

10
11 While direct imaging probably provides the best hope of finally determining the
12 structure of microporous carbon, other techniques can give valuable
13 corroborative information. We have seen that careful analysis of electron energy
14 loss spectra has revealed features that can be ascribed to five-membered rings
15 [32]. More work in this area, involving both experimental studies and
16 theoretical analysis would be welcome, as would further studies using
17 techniques such as Raman spectroscopy and X-ray and neutron diffraction.
18
19
20
21
22
23
24
25
26
27
28
29
30

31 If experimental evidence for a fullerene-related structure appears to be growing,
32 theoretical studies of the formation of microporous carbon also point in the
33 same direction. It is surely significant that four separate modelling studies, all
34 using slightly different methods and starting systems [38 - 41], each produce
35 structures containing non-hexagonal rings. Particularly notable is the
36 resemblance between the structure of Powles and colleagues (Fig. 9), and the
37 structure inferred from TEM observations shown in Fig. 5. There is clearly
38 scope for further modelling work on the evolution of carbonaceous material
39 into carbon, since there is still much that we do not understand. In particular,
40 the question of why some materials yield non-graphitizing carbon while others
41 give graphitizing carbon is not at all well understood at the molecular level.
42
43
44
45
46
47
48
49
50
51
52
53
54
55
56
57
58
59
60
61
62
63
64
65

A fullerene-like model for microporous carbon could be of great value in understanding its adsorptive properties. It is widely recognised that the slit pore model has serious deficiencies [57 - 61], and it has been known for some time that the profile for small-angle (X-ray or neutron) scattering does not correspond to the model predictions for slit scattering. However, a widely-accepted alternative model has not yet emerged. Theoretical studies by Terzyk *et al.* [42 - 49] have shown that fullerene-like models can replicate reasonably well the densities, pore size distributions and adsorption isotherms observed experimentally, and it would be valuable if other groups were to carry out similar studies. One way in which the modelling work could be extended would be by employing larger fragments. It is very difficult to determine accurately the size of the individual fragments in microporous carbon, but recent work by Kyotani and colleagues has suggested that they may be larger than generally thought [62]. In this work, the amount of hydrogen in carbon materials heat-treated to 1000°C and above was measured. The crystallite sizes were then determined by assuming that all the edge sites were terminated by hydrogen atoms. In this way it was found that a non-graphitizing carbon prepared from polyfurfuryl alcohol by heating to 1000°C had a crystallite size of 12 nm, much larger than the size estimated from X-ray diffraction (1 nm). This is understandable, since XRD measurements assume planar crystallites, and the structures in a non-graphitizing carbon are of course highly curved. A graphene crystallite with a diameter of 12 nm would contain approximately 4500 atoms, whereas the fragments employed by Terzyk *et al.* generally had fewer than 500 atoms. It is quite possible that structures constructed from larger fragments would

display similar behaviour to those made from smaller ones, but further modelling studies are needed to confirm this.

Acknowledgements

I thank Artur Terzyk and Kazu Suenaga for discussions.

References

1. Derbyshire F, Jagtoyen M, Thwaites M (1995) In: Patrick JW, editor Porosity in carbons: Characterization and applications. Edward Arnold, London p. 227
2. Patrick JW, editor (1995) Porosity in carbons: Characterization and applications. Edward Arnold, London
3. Marsh H, Rodriguez-Reinoso F (2006) Activated carbon. Elsevier, Oxford.
4. Harris PJF, Tsang SC (1997) Philosophical Magazine A 76: 667
5. Harris PJF (1997) International Materials Reviews 42: 206
6. Emmett PH (1948) Chemical Reviews 43: 69
7. Franklin RE (1951) Proceedings of the Royal Society A 209: 196
8. Lim YI, Bhatia SK (2011) Journal of Membrane Science 369: 319
9. Sitprasert C, Zhu ZH, Wang FY, Rudolph V (2011) Chemical Engineering Science 66: 5447
10. Ergun S, Tiensuu VH (1959) Acta Crystallographica 12: 1050
11. Burian A, Ratuszna A, Dore JC, Howells SW (1998) Carbon 36: 1613
12. Ban LL (1972) In: Roberts MW, Thomas JM, editors. Surface and Defect Properties of Solids, vol 1. Chemical Society, London p. 54
13. Ban LL, Crawford D, Marsh H (1975) Journal of Applied Crystallography 8: 415
14. Jenkins GM, Kawamura K (1971) Nature 231: 175

15. Oberlin A (1989) In: Thrower PA, editor. Chemistry and Physics of Carbon, vol 22, Dekker, New York p. 1-143.
16. Kroto HW, Heath JR, O'Brien SC, Curl RF, Smalley RE (1985) Nature 318: 162
17. Krätschmer W, Lamb LD, Fostiropoulos K, Huffman DR (1990) Nature 347: 354
18. Kroto HW (1992) Angewandte Chemie 31: 111
19. Iijima S (1991) Nature 354: 56
20. Harris PJF (2009) Carbon nanotube science. Cambridge University Press, Cambridge
21. Harris PJF, Tsang SC, Claridge JB, Green MLH (1994) Journal of the Chemical Society-Faraday Transactions 90: 2799
22. Iijima S, Yudasaka M, Yamada R, Bandow S, Suenaga K, Kokai F, Takahashi K (1999) Chemical Physics Letters 309: 165
23. Harris PJF, Burian A, Duber S (2000) Philosophical Magazine Letters 80: 381
24. Harris PJF (2003) In: Radovic LR, editor. Chemistry and Physics of Carbon, vol 28, Dekker, New York p. 1
25. Harris PJF (2004) Philosophical Magazine 84: 3159
26. Harris PJF (2005) Critical Reviews in Solid State and Materials Sciences 30: 235
27. Iijima S, Ichihashi T, Ando Y (1992) Nature 356: 776
28. Erni R (2010) Aberration-corrected imaging in transmission electron microscopy: An introduction. Imperial College Press, London.
29. Hashimoto A, Suenaga K, Gloter A, Urita K, Iijima S (2004) Nature 430: 870
30. Meyer JC, Kisielowski C, Erni R, Rossell MD, Crommie MF, Zettl A (2008) Nano Letters 8: 3582
31. Harris PJF, Liu Z, Suenaga K (2008) Journal of Physics-Condensed Matter 20: 362201.
32. Zhang Z, Brydson R, Aslam Z, Reddy S, Brown A, Westwood A, Rand B (2011) Carbon 49: 5049

33. El-Barbary AA, Trasobares S, Ewels CP, Stephan O, Okotrub AV, Bulusheva LG, Fall CJ, Heggge MI (2006) *Journal of Physics: Conference Series* 26: 149
34. Burian A, Dore JC (2000) *Acta Physica Polonica A* 98: 457
35. Burian A, Daniel P, Duber S, Dore JC (2001) *Philosophical Magazine B* 81: 525
36. Hawelek L, Koloczek J, Brodka A, Dore JC, Honkimaki V, Burian A (2007) *Philosophical Magazine* 87: 4973
37. Hawelek L, Brodka A, Dore JC, Honkimaki V, Burian A (2008) *Diamond and Related Materials* 17: 1633
38. Acharya M, Strano MS, Mathews JP, Billinge JL, Petkov V, Subramoney S, Foley HC (1999) *Philosophical Magazine B* 79: 1499
39. Kumar A, Lobo RF, Wagner NJ (2005) *Carbon* 43: 3099
40. Shi YF (2008) *Journal of Chemical Physics* 128: 234707
41. Powles RC, Marks NA, Lau DWM (2009) *Physical Review B* 79: 075430
42. Terzyk AP, Furmaniak S, Gauden PA, Harris PJF, Włoch J, Kowalczyk P (2007) *Journal of Physics-Condensed Matter* 19: 406208
43. Terzyk AP, Furmaniak S, Harris PJF, Gauden PA, Włoch J, Kowalczyk P, Rychlicki G (2007) *Physical Chemistry Chemical Physics* 9: 5919
44. Terzyk AP, Furmaniak S, Gauden PA, Harris PJF, Włoch J (2008) *Journal of Physics-Condensed Matter* 20: 385212
45. Furmaniak S, Terzyk AP, Gauden PA, Kowalczyk P, Harris PJF (2009). *Journal of Physics-Condensed Matter* 21: 315005
46. Furmaniak S, Terzyk AP, Gauden PA, Harris PJF, Kowalczyk P (2010) *Journal of Physics-Condensed Matter* 22: 085003
47. Terzyk AP, Gauden PA, Furmaniak S, Wesołowski RP, Harris PJF (2010) *Physical Chemistry Chemical Physics* 12: 812
48. Gauden PA, Terzyk AP, Furmaniak S, Harris PJF, Kowalczyk P (2010) *Applied Surface Science* 256: 5204
49. Furmaniak S, Terzyk AP, Gauden PA, Kowalczyk P, Harris PJF (2011) *Journal of Physics-Condensed Matter* 23: 395005
50. Bhattacharya S, Gubbins KE (2006) *Langmuir* 22: 7726

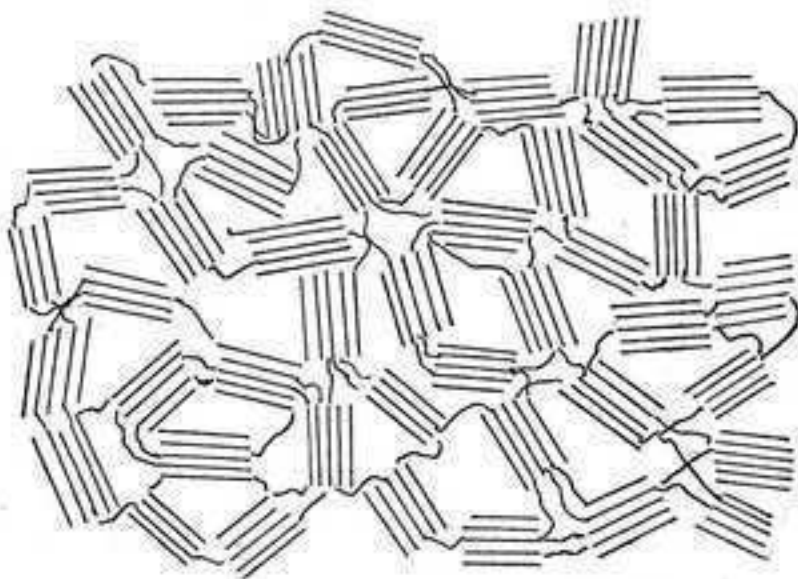
51. Yan QL, de Pablo JJ (1999) Journal of Chemical Physics 111: 9509
52. Kruk M, Jaroniec M, Gadkaree KP (1999) Langmuir 15: 1442
53. Horvath G, Kawazoe K (1983) Journal of Chemical Engineering of Japan 16: 470
54. Dubinin MM, Radushkevich LV (1947) Doklady Akademii Nauk SSSR 55: 327
55. Dubinin MM, Astakhov VA (1971) Izvestiya Akademii Nauk SSSR-Seriya Khimicheskaya 1: 5
56. Izotova TI, Dubinin MM (1965) Zhurnal Fizicheskoi Khimii 39: 2796
57. McEnaney B, Mays TJ, Chen XS (1998) Fuel 77: 557
58. Thomson KT, Gubbins KE (2000) Langmuir 16: 5761
59. Biggs MJ, Buts A, Williamson D (2004) Langmuir 20: 7123
60. Do DD, Do HD (2006) Journal of Physical Chemistry B 110: 17531
61. Palmer JC, Moore JD, Brennan JK, Gubbins KE (2011) Journal of Physical Chemistry Letters 2: 165
62. Kashiwara S, Otani S, Orikasa H, Hoshikawa Y, Ozaki J, Kyotani T (2012) Carbon 50: 3310

Figure Captions

- Figure 1 Franklin's representations of (a) non-graphitizing and (b) graphitizing carbons [7].
- Figure 2 (a) High resolution TEM image of carbon prepared by pyrolysis of sucrose in nitrogen at 1000 °C, (b) carbon prepared by pyrolysis of anthracene at 1000 °C. Insets show selected area diffraction patterns [23].
- Figure 3 Micrographs of (a) sucrose carbon and (b) anthracene carbon following heat treatment at 2300 °C [24].
- Figure 4 (a) Micrograph showing closed structure in PVDC-derived carbon heated at 2600 °C, (b) another micrograph of same sample, with arrows showing regions of negative curvature [4].

- Figure 5 Schematic illustration of a model for the structure of non-graphitizing carbons based on fullerene-like elements.
- Figure 6 Aberration-corrected HRTEM micrograph of fresh activated carbon, with arrow indicating possible pentagonal arrangement of carbon rings [31].
- Figure 7 (a) Aberration-corrected micrograph of activated carbon heated to 2000 °C. (b) Enlarged region showing pentagonal arrangement of spots. (c) Simulated image of structure shown in (d). (e) Second region showing pentagonal arrangement. (f) Simulated image of structure shown in (g) [31].
- Figure 8 Structural evolution of microporous carbon modelled by Acharya *et al.* [38]. The sequence of images (a) to (d) represent decreasing H/C ratio (or equivalently, increasing temperature).
- Figure 9 Curved sp² sheet structure produced in molecular-dynamics simulations by Powles *et al.* [41].
- Figure 10 Illustration of the construction of microporous structures S0, S16 and S35 from fullerene-related fragments. These structures are used by Terzyk *et al.* to simulate adsorption properties [42].
- Figure 11 Pore size distribution curves for some of the model structures created by Terzyk *et al.* [42].
- Figure 12 Argon adsorption isotherms for model structures [42].
- Figure 13 Illustration of the construction of micro-mesoporous structures, from the work of Terzyk *et al.* [43]. (i) shows individual fullerene-related fragments, (ii) shows a 2D structure constructed from these fragments. H0 is the initial 3D structure produced from the fragments; HC1 and HC2 were created by cutting boxes from this structure.
- Figure 14 Comparison of pore size distribution curves for the H0 structure determined using the Bhattacharya-Gubbins and the Horvath–Kawazoe method [43].

a



b

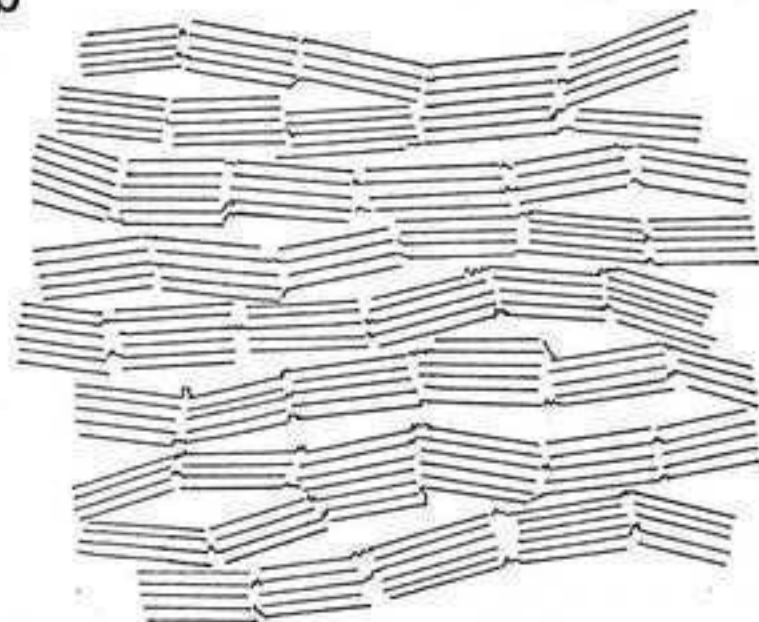


Fig. 1

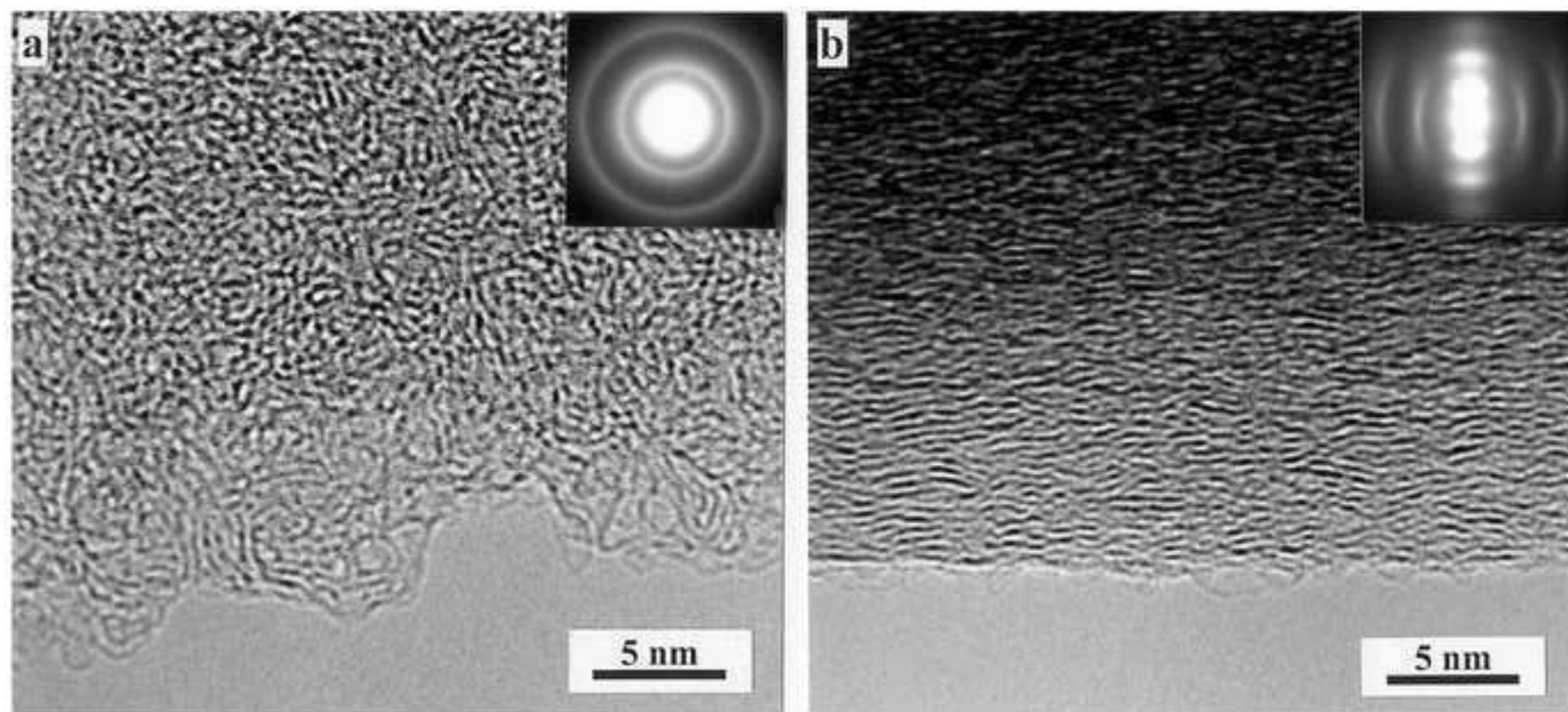


Fig. 2

Figure 3
[Click here to download high resolution image](#)

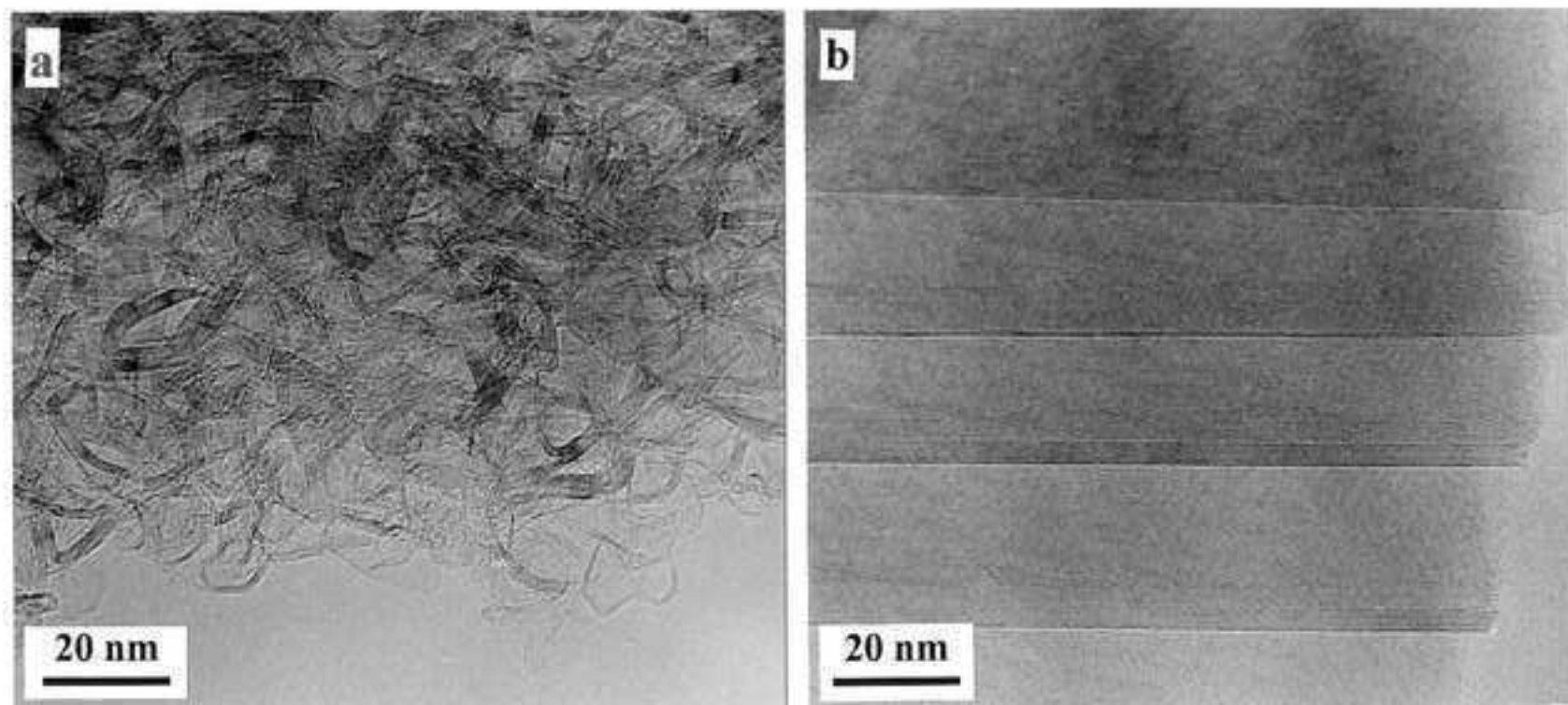


Fig. 3

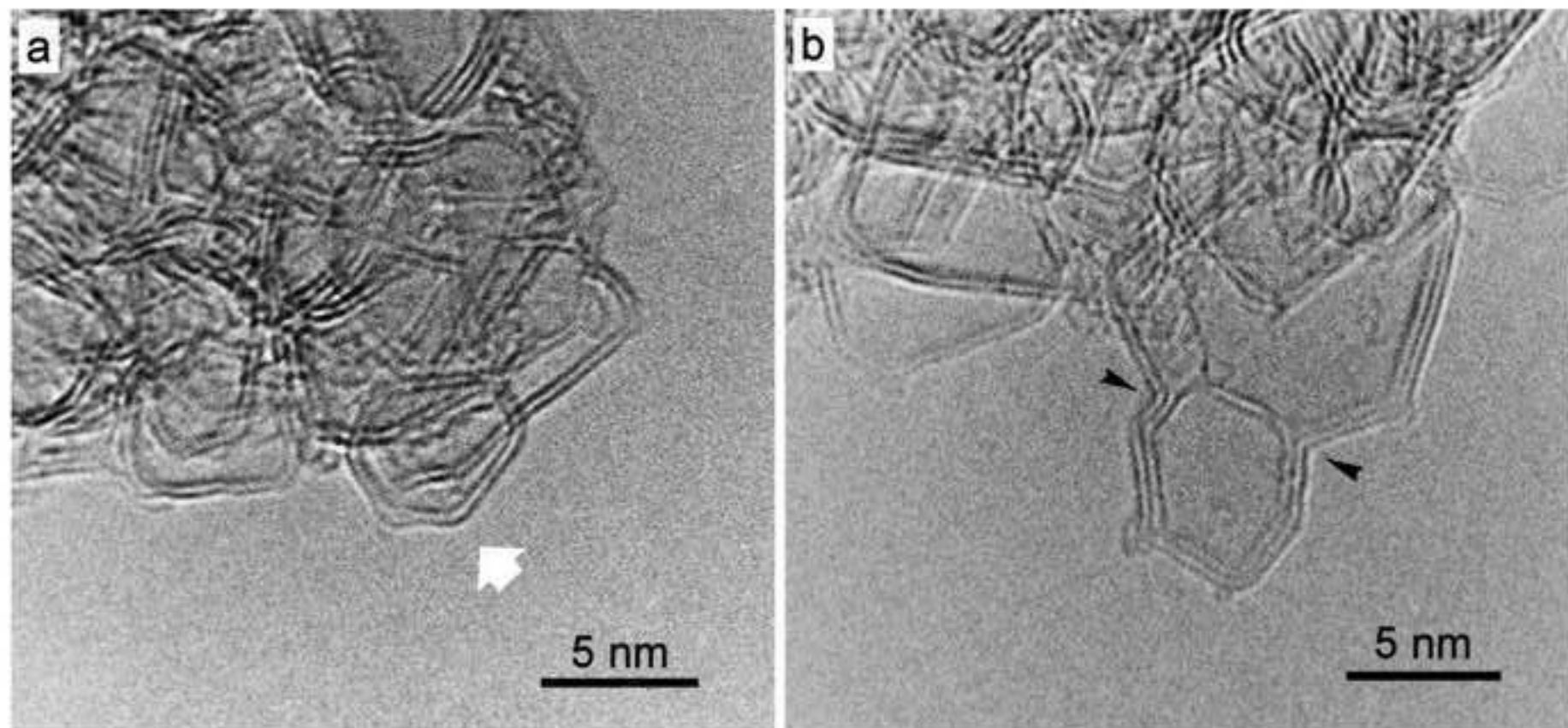


Fig. 4

Figure 5
[Click here to download high resolution image](#)

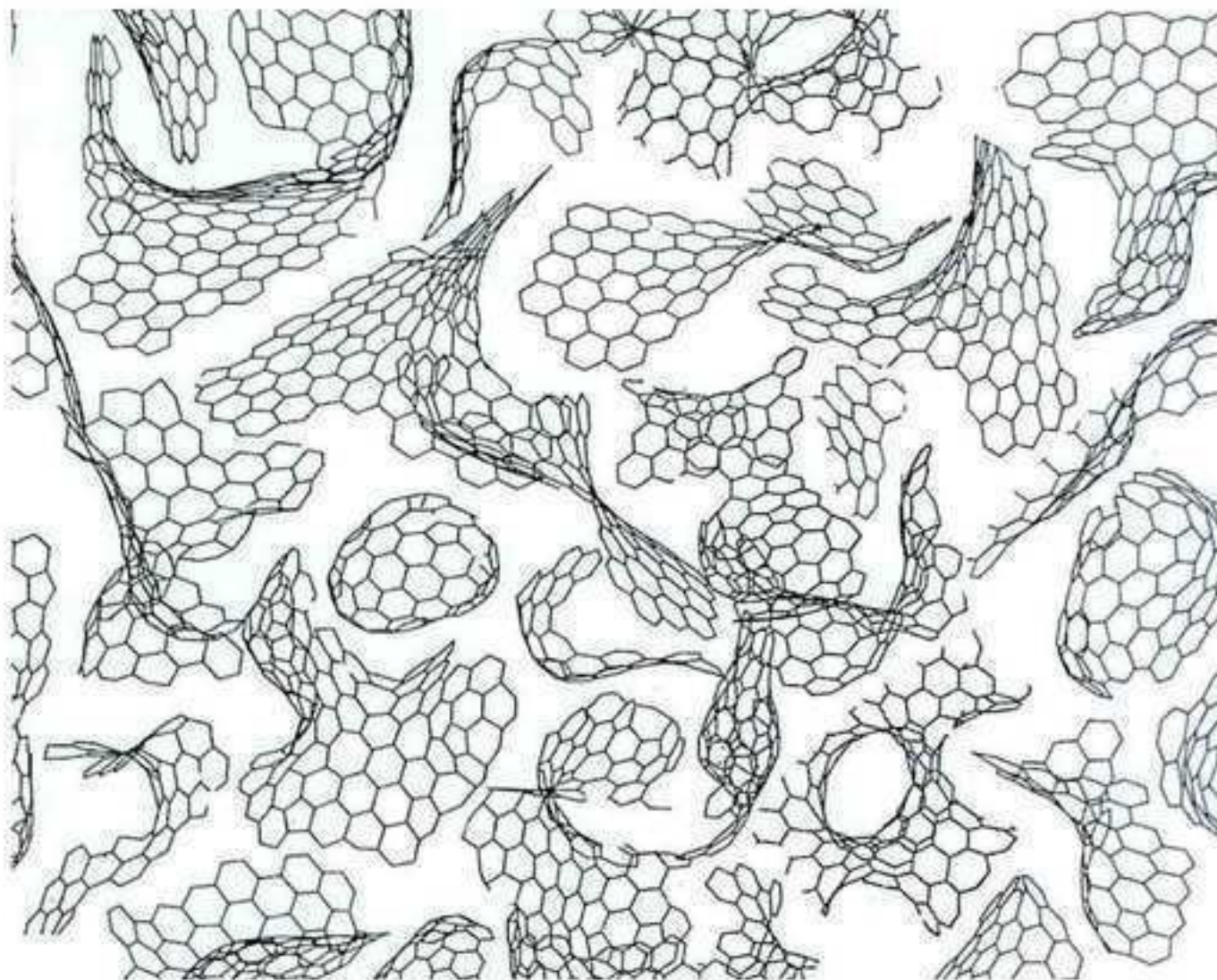


Fig. 5

Figure 6

[Click here to download high resolution image](#)

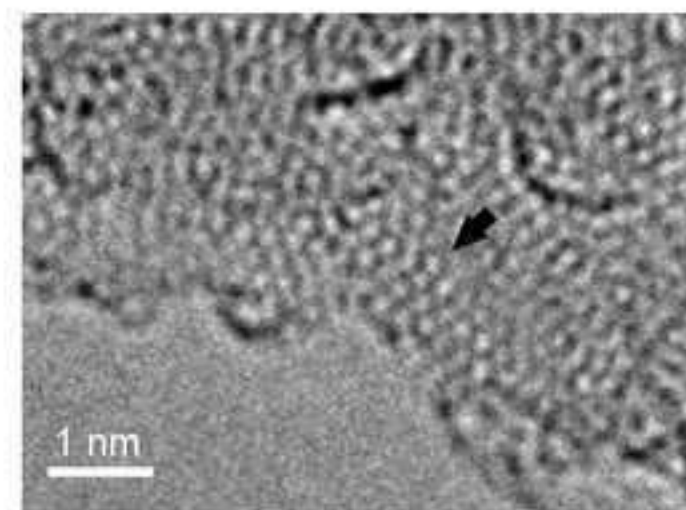


Fig. 6

Figure 7
[Click here to download high resolution image](#)

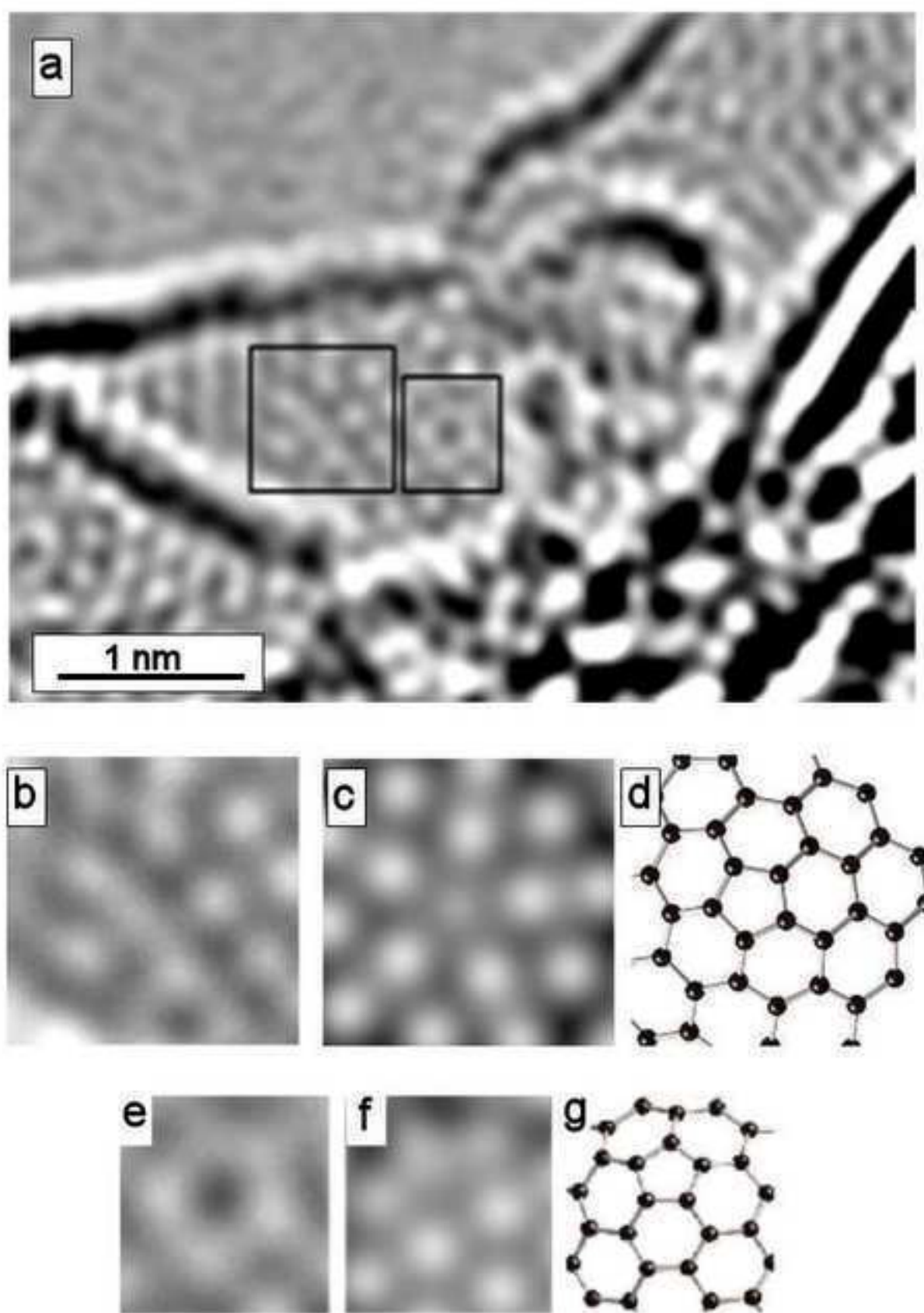
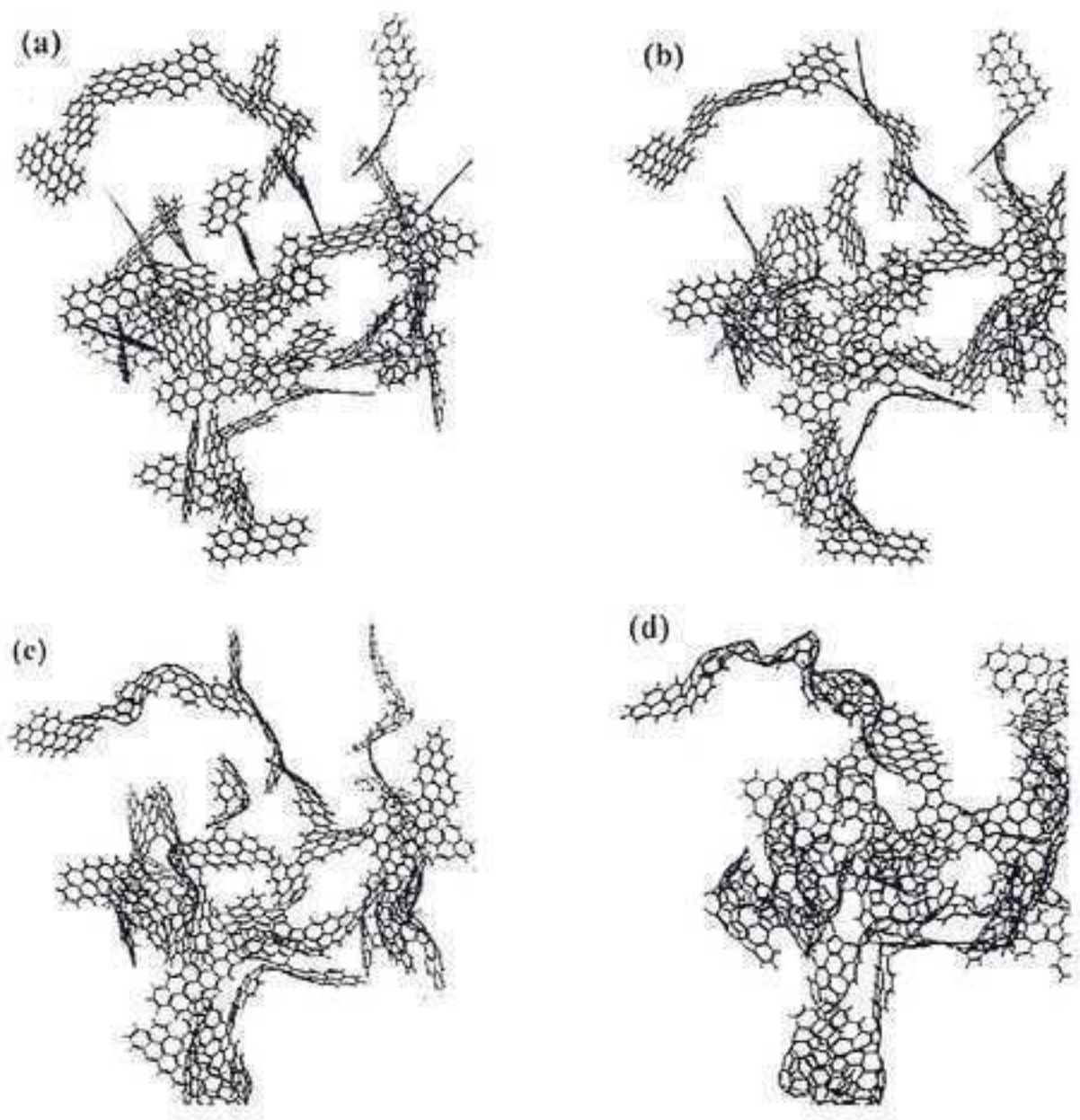


Fig. 7

Figure 8
[Click here to download high resolution image](#)



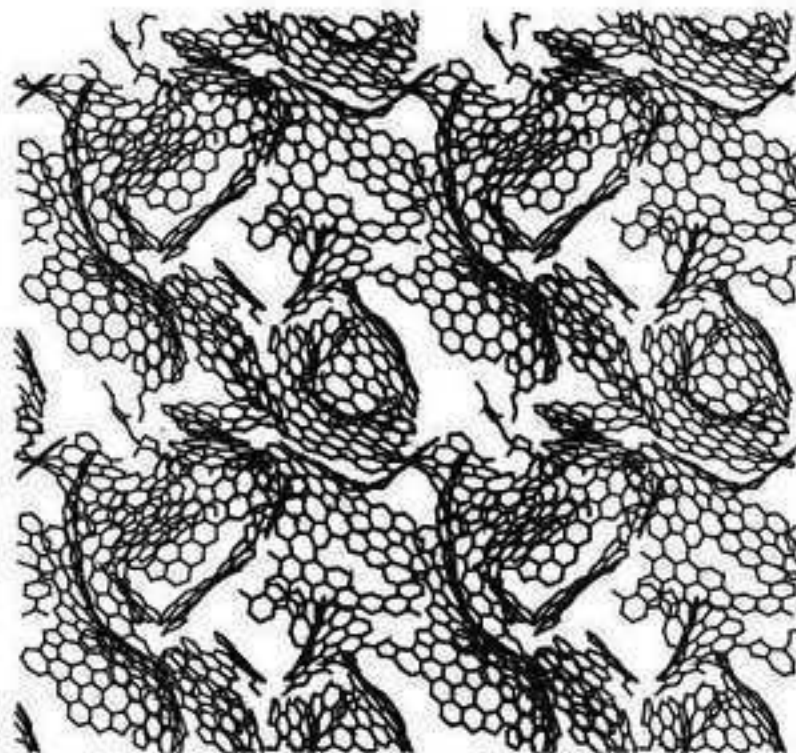


Fig. 9

Figure 10
[Click here to download high resolution image](#)

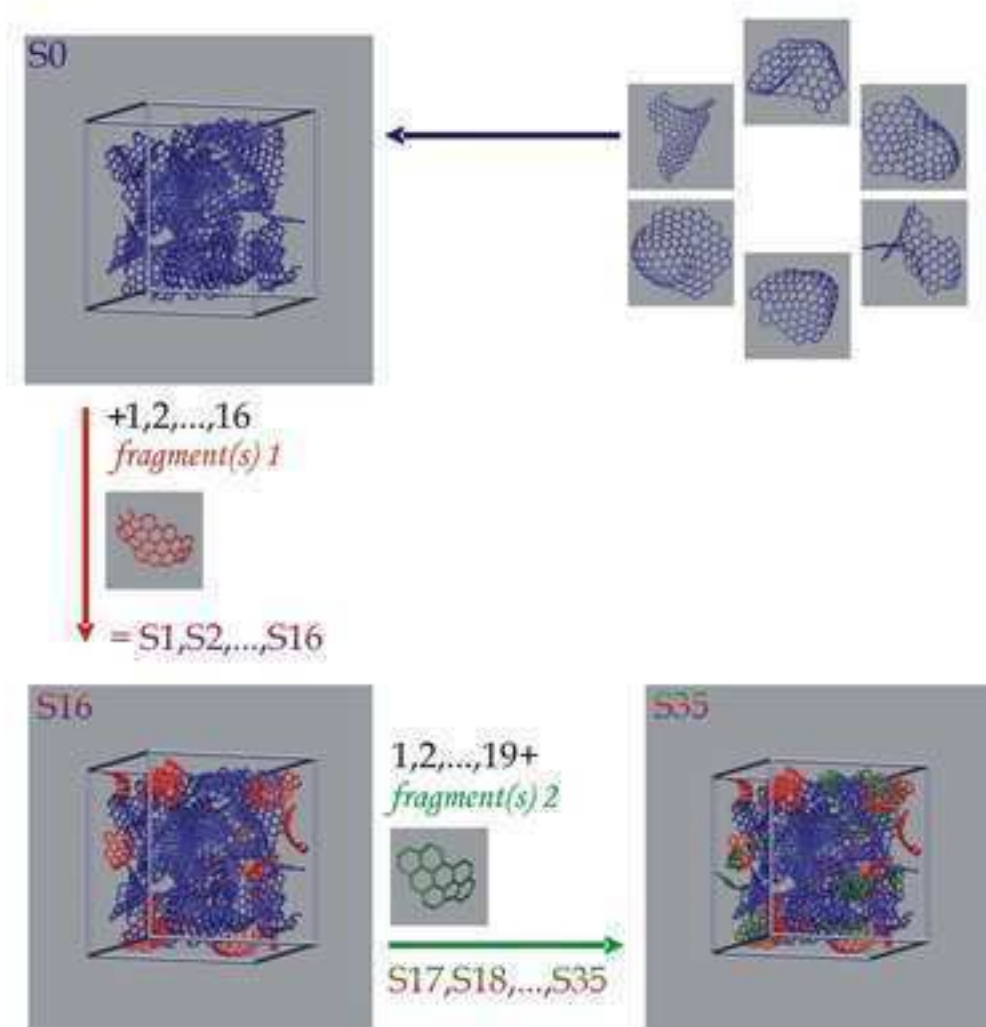


Fig. 10

Figure 11
[Click here to download high resolution image](#)

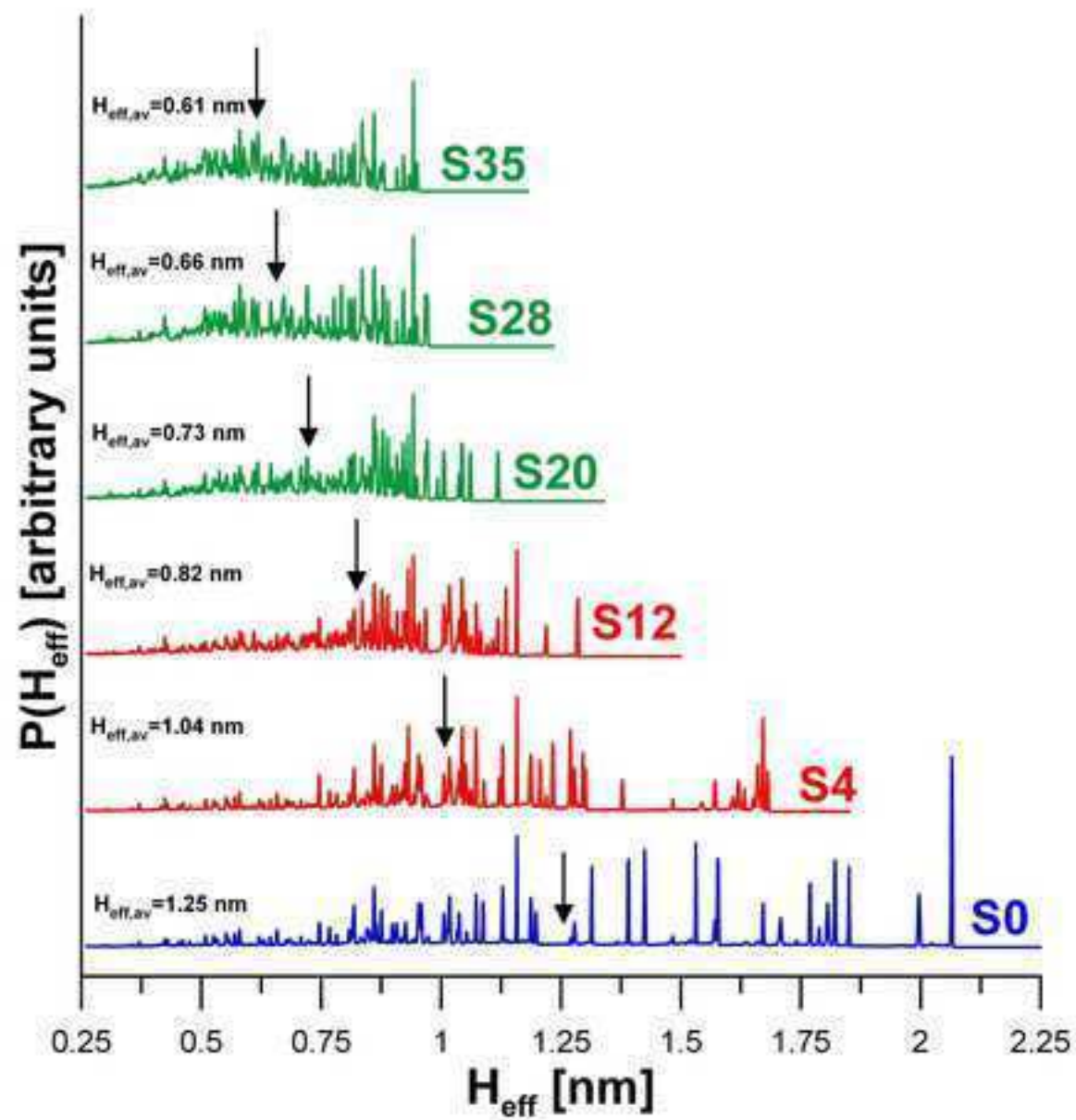


Fig. 11

Figure 12
[Click here to download high resolution image](#)

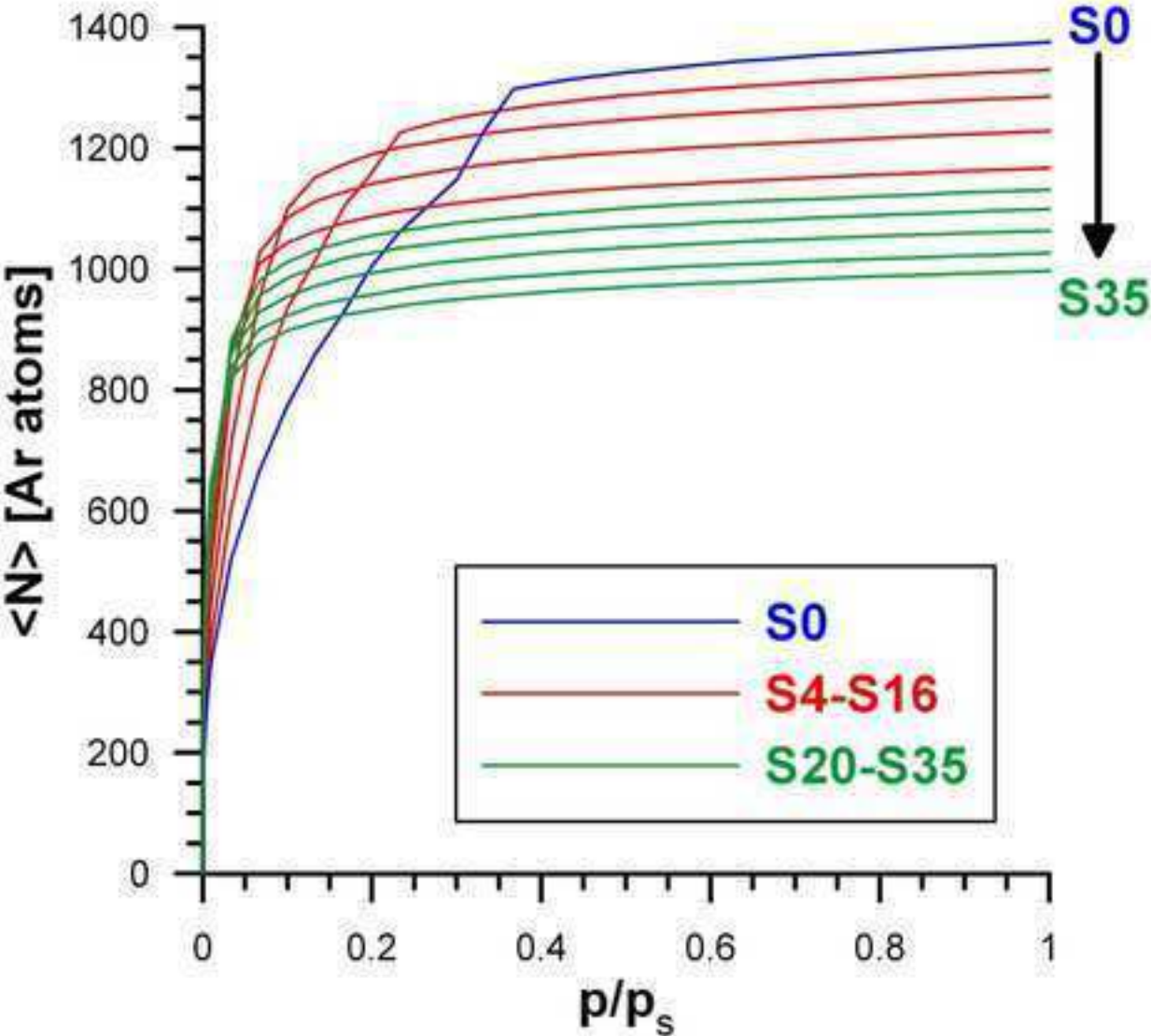


Fig. 12

Figure 13
[Click here to download high resolution image](#)

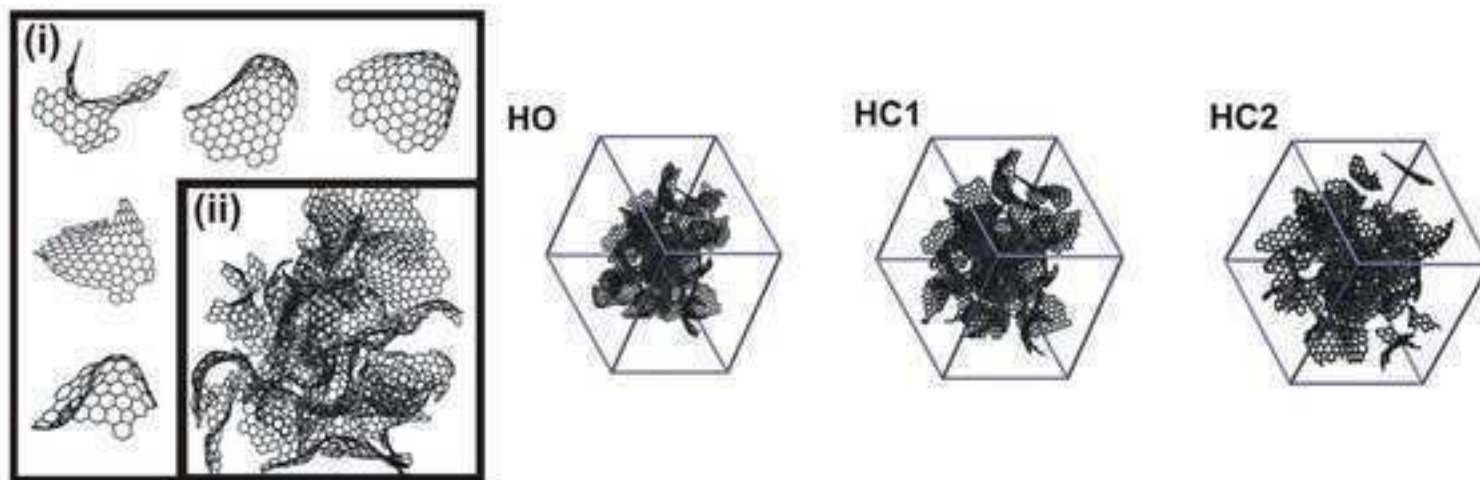


Fig. 13

Figure 14
[Click here to download high resolution image](#)

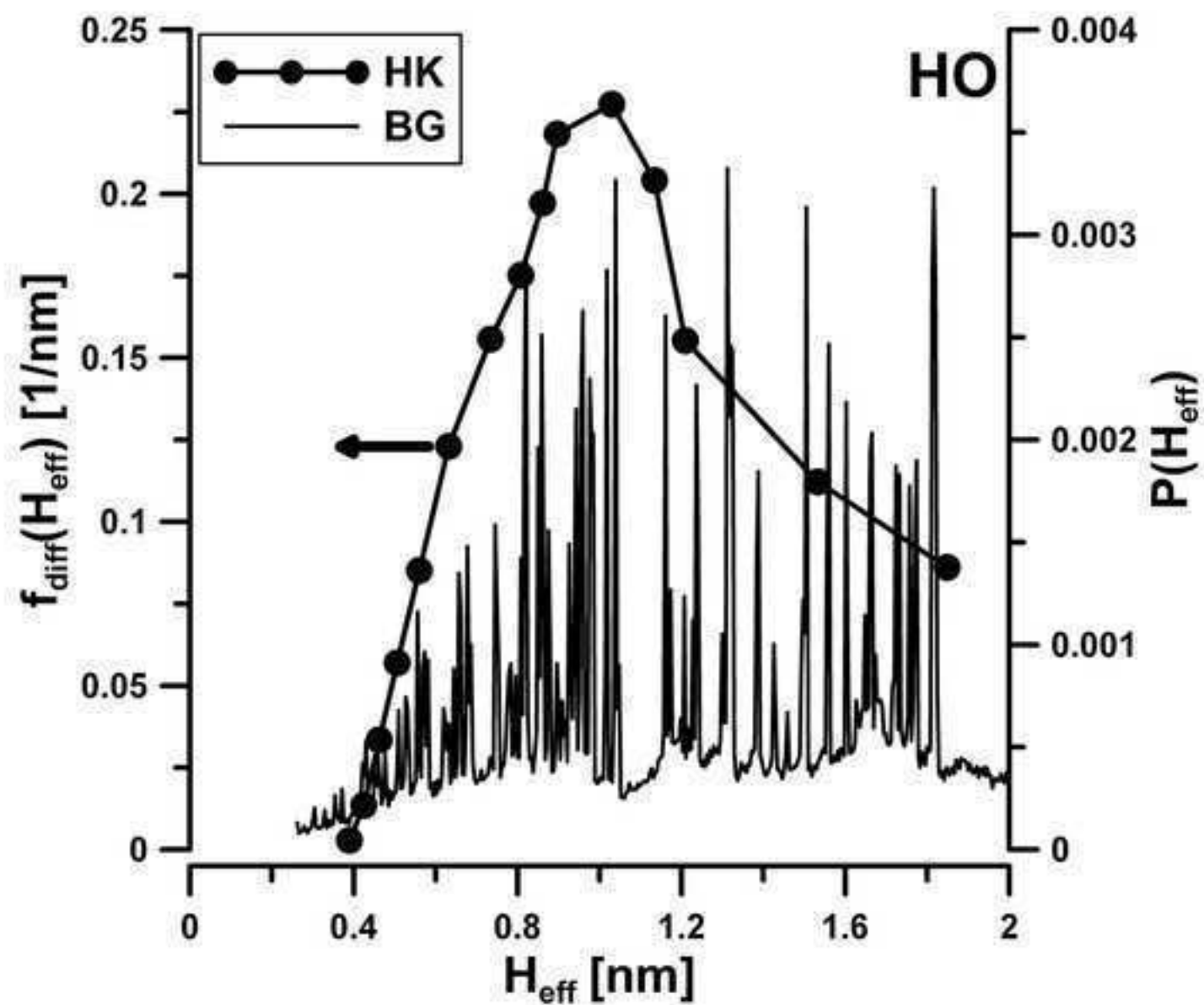


Fig. 14